

On the stochastic excitation of monostable and bistable electroelastic power generators: Relative advantages and tradeoffs in a physical system

S. Zhao and A. Erturk^{a)}

G. W. Woodruff School of Mechanical Engineering, Georgia Institute of Technology, Atlanta, Georgia 30332, USA

(Received 1 January 2013; accepted 28 February 2013; published online 13 March 2013)

Numerical and experimental investigations of broadband random vibrational energy harvesting using monostable and bistable piezoelectric cantilevers are presented along with relative performance comparisons. Simulations and experiments reveal that a linear-monostable energy harvester can outperform its bistable counterpart for very low and relatively high random excitation levels. The bistable configuration generates more power for a limited excitation intensity range slightly above the threshold of interwell oscillations. Under broadband stochastic excitation, a bistable energy harvester can potentially be preferred only if it is designed to operate at a known excitation intensity, otherwise using a monostable harvester can be more robust and practical. © 2013 American Institute of Physics. [<http://dx.doi.org/10.1063/1.4795296>]

Recent efforts by several research groups have focused on exploiting nonlinear dynamic phenomena for frequency bandwidth and performance enhancement in vibration-based energy harvesting.^{1,2} In particular, monostable^{3–7} and bistable^{8–16} nonlinear oscillators and physical systems involving such nonlinear stiffness characteristics have been subject to extensive investigation. Frequency-wise and amplitude-wise bifurcations under harmonic excitation have been well studied with demonstrations of performance enhancement by leveraging nonlinear energy harvesters provided that the preferred high-energy response is achieved (depending on the excitation level and initial conditions). Rather limited work exists on the stochastic excitation of nonlinear energy harvesters as summarized in the following, particularly to compare and clarify the relative advantages of bistable and monostable configurations.

As an early work on random vibrational energy harvesting involving nonlinearities, McInnes *et al.*¹⁷ presented a theoretical investigation of using stochastic resonance in a bistable system and suggested that the power output could be enhanced by adding periodic forcing to the white noise-type stochastic excitation. Two alternative physical bistable piezoelectric energy harvester systems (employing magnetoelastic buckling to create bistability), were contemporaneously reported by Cottone *et al.*⁸ and Erturk *et al.*⁹ in early 2009 for investigating stochastic and harmonic excitations, respectively. Cottone *et al.*⁸ and Gammaitoni *et al.*¹⁰ studied the stochastic dynamics of a bistable oscillator subjected to Gaussian random excitation, and suggested that nonlinear oscillators can outperform their linear counterparts under random excitation. Daqaq¹⁸ theoretically investigated a monostable Duffing oscillator for electromagnetic energy harvesting under white Gaussian and colored excitations, and showed that a nonlinear-monostable energy harvester does not outperform its linear counterpart under white noise excitation. Barton *et al.*¹⁹ examined a nonlinear-monostable electromagnetic

energy harvester subjected to harmonic and random excitations. Their experimental results¹⁹ were in agreement with the previous conclusion¹⁸ that the nonlinear-monostable harvester did not provide an advantage over its linear counterpart under broadband random excitation. Daqaq²⁰ provided a theoretical investigation into the response of a bistable electromagnetic energy harvester to white and exponentially correlated Gaussian noise. It was concluded that the potential shape had no influence on the expected power, so that the linear-monostable and bistable harvesters provided the same power outputs under white Gaussian noise. Litak *et al.*²¹ numerically simulated a bistable energy harvester⁹ under Gaussian white noise excitation and reported the correlation between the voltage output and standard deviation of excitation.

Although there have been comparisons of bistable and linear-monostable energy harvesters under harmonic excitation^{9,11,22} (pointing out the importance of excitation level and initial conditions to truly exploit nonlinear phenomena), the conclusions in the existing literature concerning the stochastic excitation of these two systems are lacking consistency and completeness. The aim of the present work is therefore to investigate the relative advantages of bistable and linear-monostable energy harvesters by focusing on a physical system over a wide range of noise intensity levels under broadband random excitation.

Figures 1(a) and 1(b) show schematics of typical monostable and bistable piezoelectric energy harvester configurations. In both systems, the elastic ferromagnetic cantilever is bracketed by two symmetric piezoelectric laminates at the root. The bistability in Fig. 1(b) is obtained simply by locating two magnets near the tip symmetrically following Erturk *et al.*^{9,11} (to form a piezomagnetoelastic structure based on the original magnetoelastic structure by Moon and Holmes²³). Alternative symmetric bistable beam configurations are due to Cottone *et al.*,⁸ Stanton *et al.*,¹² and Masana and Daqaq²² while an asymmetric bistable plate arrangement was investigated by Arrieta *et al.*¹⁴

The linear monostable energy harvester (Fig. 1(a)) has the dimensionless governing electromechanical equations of the following form:

^{a)} Author to whom correspondence should be addressed. Electronic mail: alper.erturk@me.gatech.edu.

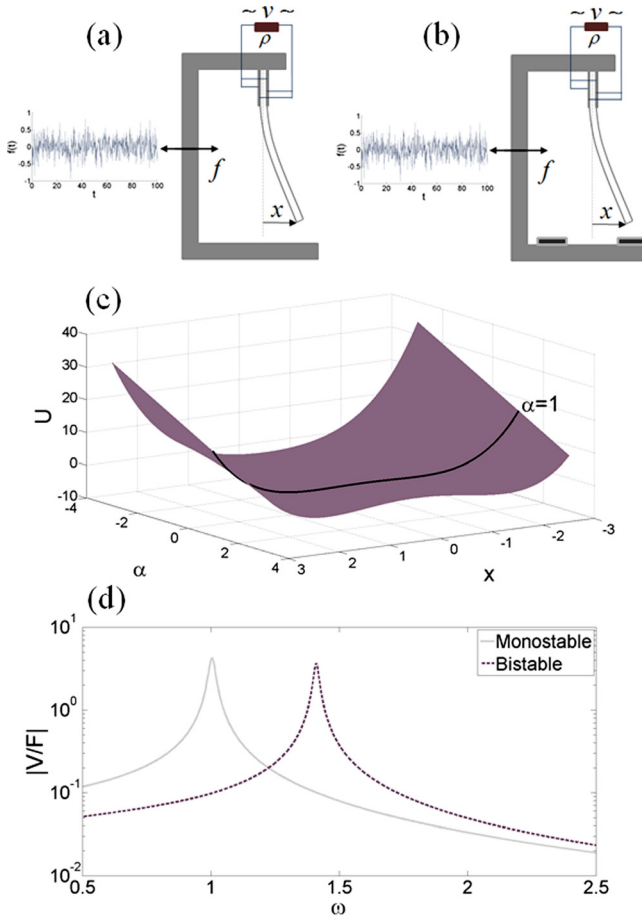


FIG. 1. Schematics of (a) monostable and (b) bistable piezoelectric energy harvesters under broadband random base excitation; (c) potential energy surface of a Duffing oscillator ($\alpha > 0$ is bistable) along with the potential energy curve of a bistable configuration with shallow potential wells ($\alpha = 1$); (d) comparison of linear FRFs of the monostable and bistable ($\alpha = 1$) configurations for small oscillations around their respective stable static equilibria ($\zeta = 0.01$, $\eta = 1$, $\theta = 0.1$, $\rho \rightarrow \infty$).

$$\ddot{x} + 2\zeta\dot{x} + x - \theta v = f(t), \quad (1)$$

$$\eta\dot{v} + v/\rho + \theta\dot{x} = 0, \quad (2)$$

where $f(t)$ is the broadband random forcing due to base excitation, $x(t)$ is the displacement response at the free end of the cantilever, $v(t)$ is the voltage output across the electrical load, η is the equivalent capacitance of the piezoelectric layers, ρ is the resistive electrical load, θ is the electromechanical coupling, ζ is the mechanical damping ratio, and an over-dot represents differentiation with respect to dimensionless time. The restoring elastic force of the linear monostable energy harvester is therefore derived from a dimensionless quadratic potential energy of the form $U(x) = x^2/2$.

A bistable energy harvester (Fig. 1(b)) has the dimensionless quartic potential energy of the form $U(x, \alpha) = -\alpha x^2/2 + x^4/4$, $\alpha > 0$; which yields the surface of Fig. 1(c) for a range of α values (both negative and positive) and displacement x . It is important to note that this surface represents the generalized potential energy of a Duffing oscillator: monostable for $\alpha < 0$ and bistable for $\alpha > 0$. The focus in this work is placed on the bistable case ($\alpha > 0$) with relatively shallow potential wells, specifically, the case of $\alpha = 1$ as depicted in

Fig. 1(c). The governing electromechanical equations of the bistable energy harvester are then

$$\ddot{x} + 2\zeta\dot{x} - x + x^3 - \theta v = f(t), \quad (3)$$

$$\eta\dot{v} + v/\rho + \theta\dot{x} = 0, \quad (4)$$

where the system parameters are as defined with Eqs. (1) and (2).

It is required to define a practical parameter representing the relative standing of monostable and bistable energy harvesters in order to correlate the simulations and experiments for qualitative comparisons. Here, the linear natural frequencies for small oscillations are taken as the bases to later correlate the numerical simulations with experiments. The linearized form of Eqs. (3) and (4) for small intrawell oscillations (due to $x = \bar{x} - 1$ or $x = \bar{x} + 1$ transformation and then linearization by assuming unchanged damping ratio) around either one of the symmetric potential wells is

$$\ddot{x} + 2\zeta\dot{x} + 2\bar{x} - \theta v = f(t), \quad (5)$$

$$\eta\dot{v} + v/\rho + \theta\dot{x} = 0. \quad (6)$$

The linear short-circuit ($\rho \rightarrow 0$, hence $v \rightarrow 0$) natural frequencies of the monostable and bistable systems are, therefore, 1 and $\sqrt{2}$, respectively. For the linear systems of Eqs. (1) and (2) and Eqs. (5) and (6), the open-circuit voltage output per force input frequency response functions (FRFs) are shown in Fig. 1(d). This picture is of importance for qualitative comparison of monostable and bistable systems in the experiments as mentioned previously.

The base excitation (vibration input) resulting in the mechanical forcing is assumed to be δ -correlated Gaussian white noise, which is a random process that ideally has a flat power spectral density (PSD). To be close to this assumption, it is ensured in the numerical simulations that the fundamental resonance frequency (the only resonance frequency in the single degree of freedom representation) is well covered with a flat PSD for both monostable and bistable configurations. The simulations in the following employ Fourier series representation of the Gaussian white noise to solve the governing first-order ordinary differential equations in a Runge-Kutta scheme.²⁴ An alternative process is to employ an Euler-Maruyama scheme to directly solve the stochastic differential equations as done by Ferrari *et al.*,¹⁵ Litak *et al.*,²¹ and Zhao and Erturk.²⁴

For a Gaussian noise process with zero mean value, the expected (mean) power output in monostable and bistable energy harvester systems is given by $E[P(t)] = \sigma_v^2/\rho$, where σ_v is standard deviation of voltage output across the load. For very low excitation levels resulting in linear random oscillations around $x = 0$ in Eqs. (1) and (2) (for the monostable case) and around $x = 1$ or $x = -1$ in Eqs. (5) and (6) (small intrawell oscillations for the bistable case), the random response energy is low and it can be shown analytically²⁴⁻²⁶ (e.g., one can use Eq. (27) in Ref. 24) that the monostable harvester can outperform the bistable one for optimal power generation (this is later visualized in Fig. 5(a)). The next two particular forcing levels that are of specific interest in the

present work are moderately low excitation that is sufficient for the bistable configuration to have random interwell oscillations (i.e., slightly above the potential barrier) and higher excitation where interwell oscillations for the bistable configuration are guaranteed (i.e., well above the potential barrier) while the monostable response is also large.

Figures 2(a) and 2(b) display two cases of typical random excitation history $f(t)$, its flat PSD for a broad range of frequencies, and comparison of the voltage output $v(t)$ versus velocity $\dot{x}(t)$ trajectories of bistable and monostable harvesters for the optimal electrical load (ρ_{opt}) of each configuration. Figure 2(a) shows simulations at a relatively low excitation level ($\sigma_f = 0.26$) for which the bistable harvester has larger electrical and mechanical responses than the monostable counterpart due to random interwell oscillations whereas Fig. 2(b) is for a higher excitation level ($\sigma_f = 0.53$) at which the monostable harvester outperforms the bistable one. It appears from Fig. 2(a) that a bistable energy harvester can outperform the monostable counterpart if the harvester (mainly its potential barrier) is designed (or tuned) for the specific excitation intensity. Although no comparison relative to the monostable counterpart was investigated, the behavior in Fig. 2(a) was formerly pointed out by Cottone *et al.*⁸ and Litak *et al.*²¹ as an advantage of the bistable configuration. For higher excitation levels, however, the monostable energy harvester outperforms the bistable one according to Fig. 2(b) even though the latter does exhibit interwell oscillations. Prior to relative comparison of the monostable and bistable configurations over the broad $\sigma_f - \rho$ range, we investigate an experimental system for qualitative verification of the trends in Fig. 2.

The experimental monostable and bistable piezoelectric energy harvester configurations are shown in Figs. 3(a) and 3(b), respectively. The monostable configuration (Fig. 3(a)) is obtained by simply removing the two magnets (Fig. 3(c)) that are symmetrically located at the tip of the bistable configuration (Fig. 3(b)). One of the two piezoelectric patches bracketing the flexible tempered steel substructure beam at

the root of the cantilever is displayed in Fig. 3(d). For small oscillations around the static equilibria of the monostable and bistable configurations, the open-circuit voltage output per base acceleration FRFs are given in Fig. 3(e). The experimental monostable and bistable systems have the linear resonance frequencies of 4.7 Hz and 7.2 Hz, respectively. Therefore, the relative standing of the bistable and monostable energy harvesters is very close to those of the numerical system described in Fig. 1 (cf. Figs. 1(d) and 3(e)). Further investigations with the experimental bistable system (not discussed here) reveal that a slight modification in the magnet spacing for static bifurcation analysis easily makes the system monostable, confirming that the potential wells of the experimental bistable harvester are indeed shallow (as in the $\alpha = 1$ case in Fig. 1(c)). Similar to the numerical case, for very low excitation levels resulting in small random oscillations around the static equilibria, the monostable system outperforms the bistable one (as later shown in Fig. 5(b)). Of particular interest are again a moderately low excitation level that results in interwell oscillations and high excitation for ensured interwell oscillations in the bistable configuration to compare with the monostable configuration.

For a base acceleration level of 0.1 g standard deviation with broad frequency content (sufficiently covering the fundamental mode), the experimentally measured electromechanical response trajectories for the optimal electrical loads of each configuration are shown in Fig. 4(a). The bistable configuration at this excitation level exhibits random interwell oscillations, and outperforms the monostable counterpart. For a base acceleration standard deviation of 0.25 g, the bistable energy harvester exhibits interwell oscillations, however, the monostable counterpart yields larger electromechanical response as displayed in Fig. 4(b). Therefore, although the bistable harvester can generate more power if carefully designed to operate at a specific random excitation intensity (slightly above the threshold of interwell oscillations), the monostable harvester generates more power for higher excitation levels even though the bistable one still

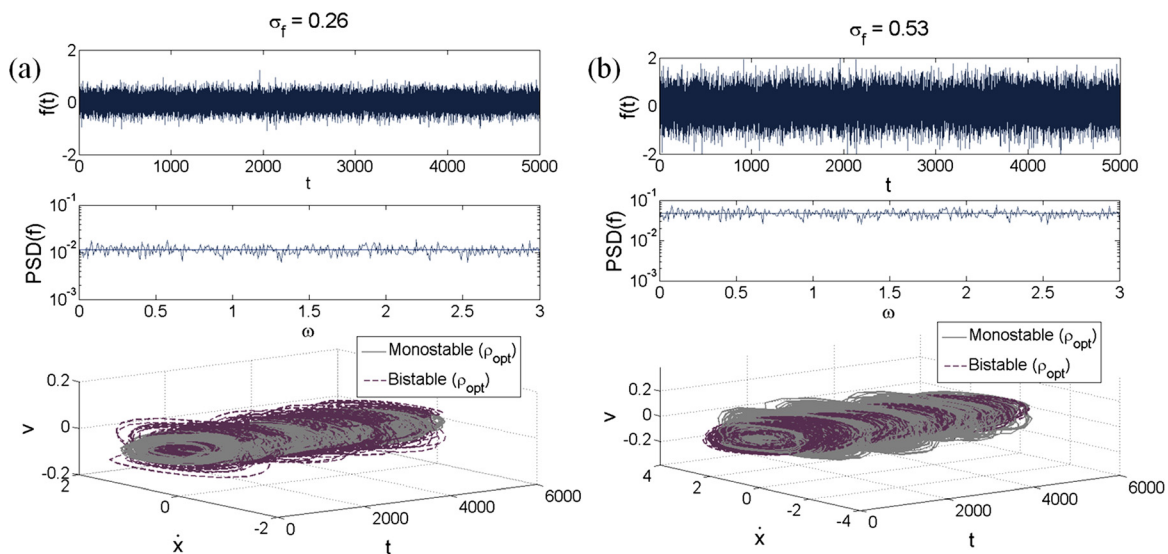


FIG. 2. Dimensionless numerical simulations for relatively (a) low ($\sigma_f = 0.26$) and (b) high ($\sigma_f = 0.53$) excitation levels of monostable and bistable energy harvesters showing the time history and PSD of the excitation force and the electromechanical response trajectories (voltage vs. velocity vs. time) for the optimal electrical load of each configuration.

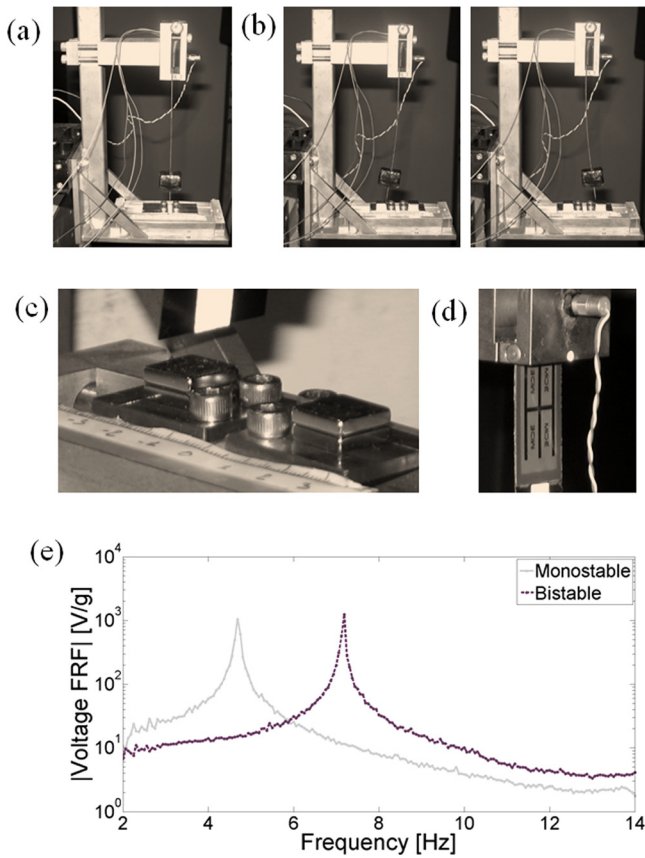


FIG. 3. Experimental (a) monostable and (b) bistable piezoelectric energy harvester configurations under horizontal base excitation (the bistable configuration is shown with its two stable static equilibria); (c) magnet arrangement at the tip of the bistable configuration; (d) detail of the piezoelectric patches at the root of the cantilever; (e) open-circuit voltage output FRFs for very small oscillations around the respective static equilibria of the monostable and bistable configurations.

exhibits interwell oscillations. Note that the experimental measurements in Fig. 4 exhibit very good agreement with the numerical results of Fig. 2.

Figures 5(a) and 5(b) present a summary of the relative performance results of linear-monostable and bistable energy

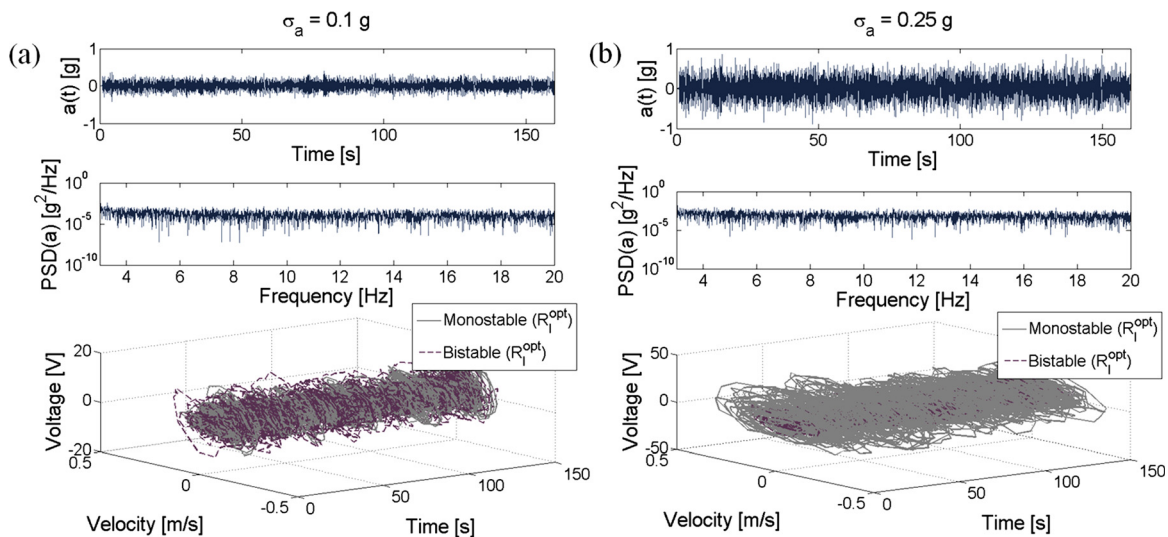


FIG. 4. Experimental results for relatively (a) low ($\sigma_a = 0.1$ g) and (b) high ($\sigma_a = 0.25$ g) excitation levels of monostable and bistable energy harvesters showing the time history and PSD of the excitation force and the electromechanical response trajectories (voltage vs. velocity vs. time) for the optimal electrical load of each configuration.

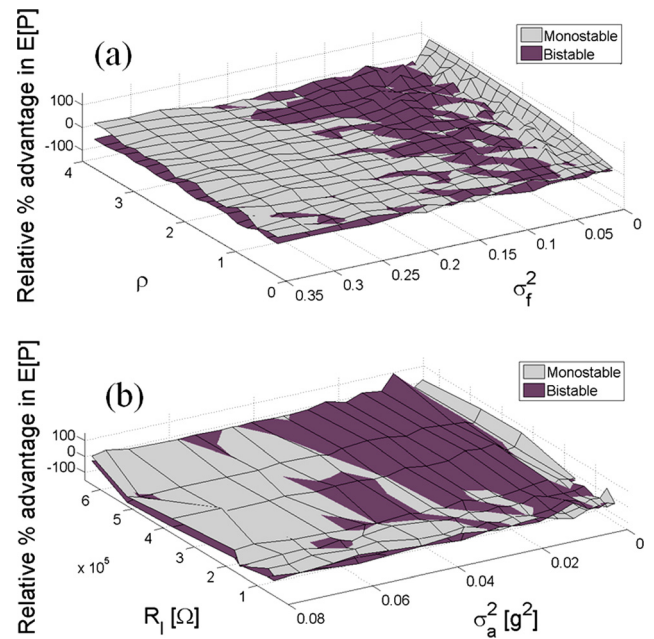


FIG. 5. (a) Numerical and (b) experimental surfaces showing the percentage advantages of the monostable and bistable energy harvesters in power generation relative to each other with changing excitation variance and load resistance (covering the optimal electrical loads of each configuration).

harvesters in power generation based on the numerical simulations and experimental measurements, respectively. Broad ranges of excitation variance and electrical load resistance are covered in Fig. 5 to draw basic conclusions. Briefly, there exist three specific excitation levels of interest: (1) very low excitation, (2) moderately low excitation (slightly above the threshold of interwell oscillations in the bistable configuration), and (3) relatively high excitation. For very low excitation levels resulting in linear oscillations around the respective static equilibria of monostable and bistable configurations, the monostable harvester outperforms the bistable one in optimal power generation. Physically the cantilever cannot escape the magnetic attraction at the respective focus in the bistable configuration (and exhibits intrawell

oscillations) whereas the monostable counterpart has no such constraint and is dynamically more flexible (cf. their resonance frequencies and relative dynamic flexibility in Figs. 1(d) and 3(e)). For moderately low excitation levels (slightly above the threshold of interwell oscillations), the bistable energy harvester can outperform its monostable counterpart due to large random response associated with interwell oscillations. This is the only neighborhood of random excitation intensity for which the bistable energy harvester can be preferred. If the excitation is relatively high, although the bistable harvester exhibits more frequent interwell oscillations than the previously discussed excitation level, the monostable counterpart generates more power output. Physically, the source of bistability (the magnetic field in this case) renders the response bounded while the linear monostable configuration has no such magnetoelastic hindering mechanism.

In summary, the numerical and experimental results reveal that a bistable energy harvester can potentially be preferred only if it is carefully designed to operate in the neighborhood of a specific random excitation intensity (requiring *a priori* knowledge of the excitation intensity level). For much lower or rather high excitation intensity levels, one should prefer to employ a linearly behaving monostable energy harvester to extract larger power output. Since there is a strong possibility of drastically reducing the power output due to imposing bistability even with shallow potential wells, it is crucial to check the available noise intensity in the application to justify the advantage of using a bistable configuration in harvesting random vibrational energy. Otherwise, if the excitation intensity is unknown, it can be more robust and practical to use a monostable configuration.

Support from the U.S. Department of Commerce, National Institute of Standards and Technology, Technology Innovation Program, Cooperative Agreement Number 70NANB9H9007, “Self-Powered Wireless Sensor Network for Structural Health Prognosis,” is gratefully acknowledged.

The authors would like to thank T. Deplace for his assistance in the experimental measurements.

- ¹L. Tang, Y. Yang, and C. K. Soh, *J. Intell. Mater. Syst. Struct.* **21**, 1867–1897 (2010).
- ²A. Erturk, *J. Intell. Mater. Syst. Struct.* **23**, 1407 (2012).
- ³B. P. Mann and N. D. Sims, *J. Sound Vib.* **319**, 515–530 (2009).
- ⁴R. Ramlan, M. J. Brennan, B. R. Mace, and I. Kovacic, *Nonlinear Dyn.* **59**, 545–558 (2010).
- ⁵B. Marinkovic and H. Koser, *Appl. Phys. Lett.* **94**, 103505 (2009).
- ⁶S. C. Stanton, C. C. McGehee, and B. P. Mann, *Appl. Phys. Lett.* **95**, 174103 (2009).
- ⁷A. Hajati and S. G. Kim, *Appl. Phys. Lett.* **99**, 083105 (2011).
- ⁸F. Cottone, H. Vocca, and L. Gammaitoni, *Phys. Rev. Lett.* **102**, 080601 (2009).
- ⁹A. Erturk, J. Hoffmann, and D. J. Inman, *Appl. Phys. Lett.* **94**, 254102 (2009).
- ¹⁰L. Gammaitoni, I. Neri, and H. Vocca, *Appl. Phys. Lett.* **94**, 164102 (2009).
- ¹¹A. Erturk and D. J. Inman, *J. Sound Vib.* **330**, 2339–2353 (2011).
- ¹²S. C. Stanton, C. C. McGehee, and B. P. Mann, *Physica D* **239**, 640–653 (2010).
- ¹³S. C. Stanton, B. A. M. Owens, and B. P. Mann, *J. Sound Vib.* **331**, 3617–3627 (2012).
- ¹⁴A. Arrieta, P. Hagedorn, A. Erturk, and D. J. Inman, *Appl. Phys. Lett.* **97**, 104102 (2010).
- ¹⁵M. Ferrari, V. Ferrari, M. Guizzetti, B. Ando, S. Baglio, and C. Trigona, *Sens. Actuators A* **162**, 425–431 (2010).
- ¹⁶L. V. Blarigan, P. Danzl, and J. Moehlis, *Appl. Phys. Lett.* **100**, 253904 (2012).
- ¹⁷C. R. McInnes, D. G. Gorman, and M. P. Cartmell, *J. Sound Vib.* **318**, 655–662 (2008).
- ¹⁸M. F. Daqaq, *J. Sound Vib.* **329**, 3621–3631 (2010).
- ¹⁹D. Barton, S. Burrow, and L. Clare, *ASME J. Vib. Acoust.* **132**, 021009 (2010).
- ²⁰M. F. Daqaq, *J. Sound Vib.* **330**, 2554–2564 (2011).
- ²¹G. Litak, M. Friswell, and S. Adhikari, *Appl. Phys. Lett.* **96**, 214103 (2010).
- ²²R. Masana and M. F. Daqaq, *J. Sound Vib.* **330**, 6036–6052 (2011).
- ²³F. C. Moon and P. J. Holmes, *J. Sound Vib.* **65**, 275–296 (1979).
- ²⁴S. Zhao and A. Erturk, *Smart Mater. Struct.* **22**, 015002 (2013).
- ²⁵E. Halvorsen, *J. Microelectromech. Syst.* **17**, 1061–1071 (2008).
- ²⁶S. Adhikari, M. Friswell, and D. J. Inman, *Smart Mater. Struct.* **18**, 115005 (2009).